Journal of Rehabilitation in Civil Engineering 6-1 (2018) 70-87

journal homepage: http://civiljournal.semnan.ac.ir/

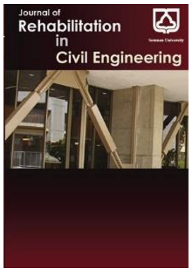

Hybrid Improved Dolphin Echolocation and Ant Colony Optimization for Optimal Discrete Sizing of Truss Structures

M. Arjmand[1], M. Sheikhi Azqandi[2*] and M. Delavar[3]

1. Department of Civil Engineering, Bozorgmehr University of Qaenat, Qaen, Iran
2. Department of Mechanical Engineering, Bozorgmehr University of Qaenat, Qaen, Iran
3. Department of Civil Engineering, Birjand University, Birjand, Iran

Corresponding author: *mojtabasheikhi@buqaen.ac.ir*

ARTICLE INFO

Article history:
Received: 17 May 2017
Accepted: 05 September 2017

Keywords:
Hybrid Optimization Algorithm,
Metaheuristic,
Discrete Variables,
Dolphin Echolocation.

ABSTRACT

This paper presents a robust hybrid improved dolphin echolocation and ant colony optimization algorithm (IDEACO) for optimizing the truss structures with discrete sizing variables. The dolphin echolocation (DE) is inspired by the navigation and hunting behavior of dolphins. An improved version of dolphin echolocation (IDE), as the main engine, is proposed and uses the positive attributes of ant colony optimization (ACO) to increase the efficiency of the IDE. Here, ACO is employed to improve the precision of the global optimization solution. In the proposed hybrid optimization method, the balance between exploration and exploitation process was the main factor to control the performance of the algorithm. IDEACO algorithm performance is tested on several problems of benchmarks discrete truss structure optimization. The results indicate the excellent performance of the proposed algorithm in optimum design and rate of convergence in comparison with other metaheuristic optimization methods, so IDEACO offers a good degree of competitiveness against other existing metaheuristic methods.

1. Introduction

The process of minimizing or maximizing an objective function is called optimization. In general, structural optimization is divided into three main types [1]. Sizing optimization, finding the area of each member of the structure. Shape (geometry) optimization, determining the coordinate nodes of the structure. Topology optimization was related to connectivity of structural members. In most cases, the three-mentioned type optimization problem is investigated independently; however, in some problems sizing; shape and topology optimization was preformed simultaneously that is called multi modals optimization [2].

Structural optimization problems can be divided into two general categories of continuous and discrete design variables. Most-recent papers on optimal structural

DOI: 10.22075/JRCE.2017.11367.1186

problems have studied with continuous design variables [3]. However, the accessibility of standard member sizes in the steel production sector proposes to select cross-sectional areas from an available list of discrete values. Optimization problems with discrete design variables are far more difficult to solve than problems with continuous [4].

Metaheuristic optimization methods are quite powerful and suitable for obtaining the solution to structural engineering optimization problems. The formulations of these methods are often inspired by either physical laws or natural phenomena. Meta-heuristic optimization methods consist of two phases: an exploration of the search region and exploitation of the best points found.

One of the main properties in extending an effective metaheuristic algorithm is to manage a suitable balance between exploration and exploitation [5-6].

Some of the popular meta-heuristic methods are such as genetic algorithms [7], simulated annealing optimization [8], ant colony optimization [9], particle swarm optimization [10], water cycle algorithm [11], min blast algorithm [12] and Time evolutionary optimization [13].

Each of the proposed optimization methods has specific characteristics. If the strengths and weaknesses of each method have been identified, they can be enhanced by combining two or more algorithms to reinforce the strengths and resolve the weaknesses of them. For this purpose, recently, the researchers have focused on the combination of optimization techniques. Some hybrid optimization algorithms are particle swarm optimizer, ant colony strategy and harmony search [14], charge system search and particle swarm optimization [15], imperialist competitive and ant colony algorithm [16], water cycle and min blast algorithm [17], particle swarm optimization and convex approximation [18], colliding bodies optimization and particle swarm optimization [19], hybrid big bang crunch [20].

Dolphin echolocation is the newly meta-heuristic algorithm proposed by Kaveh and Farhoudi [21]. DE was mimicked from strategies applied by dolphins for their hunting process.

The main advantages of the dolphin echolocation algorithm are simple formulation and no essential parameter tuning. Trapping in local optima solution at the exploitation phase is one of the weaknesses of dolphin echolocation. In the present paper, for resolving this issue, at first a version of improved dolphin echolocation was proposed, and then it was combined with ant colony optimization. The efficiency of this hybrid approach is evaluated by solving a constrained classical benchmark.

2. Discrete Structural Optimization Problems

2.1. Problem Formulation

In discrete sizing optimization of truss structures, the cost function is to minimize the total weight of the structure. The design variables are the cross-sectional area of the truss members. The optimal design must satisfy constraints such as stress and/or displacement on the structural elements and nodes, respectively.

The optimization problem for truss structures can be formulated as Eq. 1.

$$Minimize: W(A) = \sum_{i=1}^{N} \rho_i A_i L_i$$
$$Subjectto: \begin{cases} \sigma_j^{min} \le \sigma_j \le \sigma_j^{max}, j = 1,2,\dots,N \\ \delta_k^{min} \le \delta_k \le \delta_k^{max}, k = 1,2,\dots,M \\ A_r \epsilon \{\boldsymbol{S}\}, r = 1,2,\dots,N \\ \boldsymbol{S} = \{s_1, s_2, \dots, s_p\} \end{cases} \quad (1)$$

Where W is the total weight of the structure. ρ_i, A_i and L_i are the structural weight, material density, cross-sectional area, and length of the ith member, respectively. N and M are the numbers of elements and nodes of truss structure respectively

$\sigma_i$is stress in ith member and δ_i is nodal displacement in the ith node. The superscript *max* and *min* denote the maximum and minimum limits. Each cross-sectional area must be selected from a discrete set S of p available cross-sections according to production standards.

2.2. Constraint Handling

The most common strategy in the heuristic methods to handle constrains is to apply penalty functions [25]. In this method, a constrained optimization problem was converted into an unconstrained one by multiplying a coefficient penalty by cost function based upon the value of constraint violation appears as a problem. For that reason, the pseudo cost function should be transformed into Eq. 2.

$$W_p(A) = \left[(1 + \epsilon(\sum_{i=1}^{k} Max\{0, c_i(A)\})) \right]^2 W(A)$$
$$c_i(A) = \frac{g_i(A)}{g_i^{all}} - 1 \quad (2)$$

Where W_p is pseudo cost function. ϵ is constant-coefficient depending on each problem. k, $g_i(A)$ and g_i^{all} are the number of constraints, ith constraint function consist of stress or/and nodal displacement and allowable values of constraint, respectively.

3. Improved Dolphin Echolocation and Ant Colony Optimization

3.1. Dolphin Echolocation Optimization

Dolphin echolocation algorithm is a new robust, and efficient Metaheuristic algorithm for solving structural optimization problems. DE is used as a simple formulation and doesn’t need extensive mathematical computations and parameter tuning. It is widely applied to various fields of optimization problems. The flowchart of the DE algorithm was illustrated in Figure 1. It can be referred to [21] for more details about this algorithm.

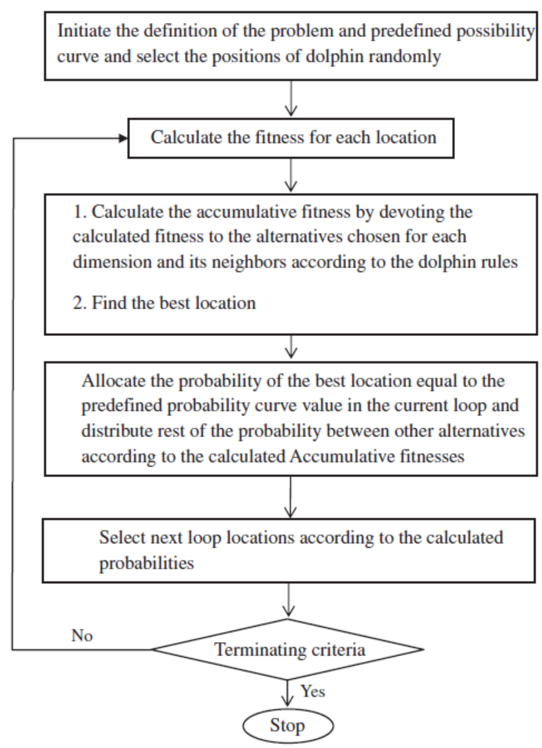

Fig. 1. The flowchart of dolphin echolocation [21].

3.2. Ant Colony Optimization

Ant colony optimization (ACO) is a metaheuristic optimization method that was originated by Dorigo *et* al. [9]. The inspiring origin of this algorithm is the behavior of real ant colonies. At first, ants explore the surrounding environment of their nest randomly. On the move, ants spatter pheromone trail on the land. As soon as an ant finds a food source, it appraises the quality and the quantity of the food and carries some of them to the nest. While moving to the nest, the amount of pheromone that an ant spatters on the land can depend on the quality and quantity of the food. The pheromone instructs other ants to the food origin. It has been shown in that the indirect communication between the ants by pheromone enable them to find the shortest paths between their nest and food sources. These abilities of real ant colonies are exploited in artificial ant colonies for solving engineering problems [24]. It can be referred to [5] for more details about ACO.

3.3. Hybrid Improved Dolphin Echolocation and ant Colony Optimization

In this section, at first an improved version of the DE was proposed, and then a hybrid optimization algorithm was presented using improved dolphin echolocation and ant colony optimization. IDE optimization was introduced, which has been improved to get the best convergence and more reliable, optimal designs, especially in the final iterations and explore best results than previous studies.

IDEACO is a new hybrid improved dolphin's echolocation and ant colony optimization algorithm. This algorithm applies to improved dolphin's echolocation for exploration of feasible space, while ant colony optimization is used as the exploitation of the best design.

The main steps of IDEACO for discrete optimization are summarized as follows:

Step 1**.** Create the alternative matrix

First, the entire search space is considered to the matrix *A*. The elements of this matrix consist of the value of allowable that can be assigned to design variables as follows Eq. 3.

$$A_{(m,n_{var})} = \begin{bmatrix} A_{1,1} & A_{1,2} & \cdots & A_{1,j} & \cdots & A_{1,\mathrm{nvar}} \\ A_{2,1} & A_{2,2} & \cdots & A_{2,j} & \cdots & A_{2,\mathrm{nvar}} \\ \vdots & \vdots & \ddots & \vdots & \ddots & \vdots \\ A_{i,1} & A_{i,2} & \cdots & A_{i,j} & \cdots & A_{i,\mathrm{nvar}} \\ \vdots & \vdots & \ddots & \vdots & \ddots & \vdots \\ A_{m,1} & A_{m,2} & \cdots & A_{m,j} & \cdots & A_{m,\mathrm{nvar}} \end{bmatrix} \quad (3)$$

Where m and n_{var} are the number of alternative and design variables, respectively. Elements of the matrix on each column are sorted from less to more.

Step 2. Create initial population

To start the optimization algorithm, matrix *L* is a candidate representing a matrix of the initial population with size ($n_{pop}\times n_{var}$), which was produced randomly from matrix *A* as follows:

```
for j=1 to the number of design variables
  for i=1 to the number of population
    L(i,j) = A(randi(m), j);
  end
end
```

$$L = \begin{bmatrix} L_{1,1} & L_{1,2} & \cdots & L_{1,j} & \cdots & L_{1,n_{var}} \\ L_{2,1} & L_{2,2} & \cdots & L_{2,j} & \cdots & L_{2,n_{var}} \\ \vdots & \vdots & \cdots & \vdots & \cdots & \vdots \\ L_{i,1} & L_{i,2} & \cdots & L_{i,j} & \cdots & L_{i,n_{var}} \\ \vdots & \vdots & \cdots & \vdots & \cdots & \vdots \\ L_{n_{Pop},1} & L_{n_{Pop},2} & \cdots & L_{n_{Pop},j} & \cdots & L_{n_{Pop},n_{var}} \end{bmatrix} \quad (4)$$

Where n_{pop} is the number of population.

Step 3. Calculate the fitness of each population

Fitness must be defined in a manner that better solutions get higher values. In other hands, by decreasing the objective function (*f(x)*), the fitness ($Fitness$) must be increased. In this paper, fitness is specified as Eq. 5.

$$Fitness = \frac{\beta}{f(x)} \tag{5}$$

Where *f(x)* is an objective function, β is constant-coefficient that is depended upon the type of problem that has value 10e3 in this paper.

Step 4. Sort the matrix *L*

The rows of matrix *L* based upon the fitness was sorted descending that is called *SL*. The fitness array of *SL* is *SFitness* as follows:

```
[SFitness, indF ] = sort(Fitness,1,'descend');
for j =1 to the number of design variables
  for i=1 to the number of population
    SL(i,j)=L(indF(i),j);
  end
end
```

Step 5. Calculate the effective radius

The fitness of each member's matrix *SL* is distributed by radius (R_i) of them. The value of R_i depends upon the radius of the main loop (R_M), number of iteration ($Iter$ and $Iter_{max}$) and the place of each member on matrix *SL*, (i) as Eq. 6. to Eq. 7.

$$R_i = \left[R_M - (R_M - 1)\left(\frac{i}{n_{Pop}}\right)\right], i = 1, \dots, n_{pop} \tag{6}$$

Where i denotes to each member of the matrix *SL*. R_M is determined by Eq. 5.

$$R_M = \left[R_{max} - (R_{max} - R_{min})\left(\frac{Iter}{Iter_{max}}\right)\right] \tag{7}$$

Where R_{max}, R_{min}, *Iter,* and $Iter_{max}$ are the maximum and minimum of R_M, the number of iteration in optimization procedure and the maximum number of iteration, respectively. R_{max}, R_{min} was selected according to the size of the search space. In this paper, the values of R_{max} and R_{min} are considered ¼ to ¾ of the number of alternative matrices and 2 or more than it.

Step 6. Calculate the accumulative fitness

After the calculation of R_i, the members of the matrix *SL* found from matrix *A* and then accumulative fitness (*AF*) is calculated as follows (Eq. 8.):

$$AF(a+k,j) = \varphi\left(\frac{R_i - abs(k)}{R_i}\right)SFitness(i) + AF(a+k,j) \tag{8}$$

Where φ is calculated by Eq. 9.

$$\varphi = \frac{1}{i^2} \tag{9}$$

```
for i=1 to the number of population
  for j =1 to the number of design variables
    find the place of SL(i,j) in jth column matrix A and
      called a
      for k=-Ri to Ri
        calculate AF (a+k, j) by Eq. 8.
      end
  end
end
```

By increasing the amount of i, the fitness of each population of the matrix *SL* is decreased. Parameter φincreases this effect.

Accumulative fitness was distributed linearly. Figure 2 shows the distribution and their overlaps and reflects on the lower and upper bound of the design's variables as follows:

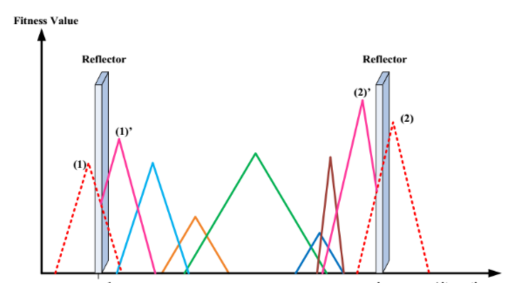

Fig. 2. the distribution of accumulated fitness [22].

```
for j=1 to the number of design variables
  for i=1 to the number of population
    a=find(A(:,j)==SL(i,j));
 %Calculate the radius of each member of the matrixSL
    Ri=Max(floor(RM-(RM-1)*i/npop),1);
    for k=-Ri to Ri
      if a+k<1
        S=abs(a+k)+1;
      else if  a+k>size(A,1)
       S=2*size(A,1)-(a+k)+1;
      else
        S=a+k;
```

```
      end
      AF(S,j)=(1/R_i)*(1/i^2)*(R_i-
        abs(k))*(SFitness(i))+AF(S,j);
    end
  end
end
```

Step 7: Obtain the best answers and create *BestL* matrix

The best solutions obtained, until now, is saved in *BestL* matrix. Matrix rows of *BestL* are sorted based on their fitness. The top rows of this matrix have a bigger fitness, so the first row of this matrix is the best optimal designs among the other rows. *BestF* is the array of the fitness of the matrix *BestL*.

BestL is a memory which saves some historically best design and can improve the algorithm performance, such as higher rate convergence without increasing the computational cost [23].

Step 8. Calculate the effective parameters for increasing accumulative fitness on *BestL*

In this step, by using the properties of ant colony optimization on continuous variables [24], the accumulative fitness of members in *BestL* is increased. For this purpose, parameter ω is defined as Eq. 10.

$$\omega_i = \left(\frac{1}{q\sqrt[2]{2\pi}} e^{-\frac{(i-1)^2}{2q^2}}\right), i = 1, \dots, n_{pop} \quad (10)$$

Where i is each member of the population. q is defined as Eq. 11.

$$q = K\left(1 - \left(\frac{Iter}{Itermax}\right)^{Pow}\right) + \varepsilon \quad (11)$$

Where K made more uniform, the amount of q and calculated by Eq. 10. *Pow* is dependent on the problem that has a value between 0.1 and 2. *Pow* and constant parameter ε are 0.4 and 1e-6, respectively.

$$K = \frac{fitness\ of\ best\ solution\ in\ all\ iterations}{fitness\ of\ best\ solution\ in\ current\ iteratio} \quad (12)$$

Step 9. Calculate the enhance probability of *BestL* in accumulative fitness matrix

The values of members in the accumulative fitness matrix are increased based on *BestL* as follows:

```
for j=1 to the number of population
  for i=1 to the number of design variables
    RS=Rand-selection in jth column of BestL
    X=find a row of RS in matrix A
    Calculate AF (X, j) by Eq. 13.
  end
end
```

$$AF(X,j) = \left(AF(X,j) + \frac{BestF(RS)}{RS}\right)N \quad (13)$$

Where N is calculated from Eq. 12.

$$N = 1 + \omega \quad (14)$$

In equations 10 to 14, by increasing coefficient i, factors ω and N will increase.

In Eq. 13, $\frac{BestF(RS)}{RS}$ prevents the members of the matrix *AF* is zero. In addition, this term led to the algorithm can be escaped from the local minimum optimal.

Step 10. Calculate the probability of each member of matrix *A*

The probability of each member matrix *A* is calculated according to the accumulative fitness matrix by Eq. 15.

$$P_{i,j} = \frac{AF_{i,j}}{\sum_{i=1}^{n_{Alt}} AF_{i,j}}, \quad j = 1,2,\dots,n_{var}, \quad i = 1,2,\dots,n_{Alt} \quad (15)$$

Step 11. Rearrange the matrix*L*

The new matrix *L* is created by roulette wheel according to matrix *P*, as follows:

```
for i=1 to the number of design variables
  for j=1 to the number of population
    r=rand;
    C(:,j)=(P(:,j))/(sum(P(:,j)));
    C(:,j)=cumsum(C(:,j));
    F=find(C(:,j)>=r,1,'first');
    L(i,j)=A((F),j);
  end
end
```

Steps 3 to 11 are repeated as many times as stop criteria is satisfied.

The flowchart of IDEACO is shown in Figure3. In this flowchart, the blue step is obtained from ant colony optimization.

In main steps mentioned about IDEACO, steps 4, 7 and 9 are added, and steps 5, 6 and 10 included modified effective radius, accumulative fitness, and probability of selection, are improved compared to algorithm DE optimization.

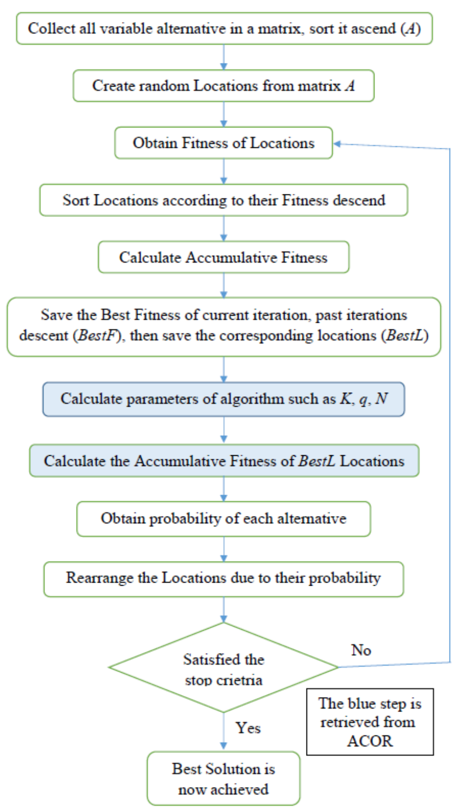

Fig. 3. The flowchart of IDEACO algorithm.

4. Design Examples

The performance of the proposed meta-heuristic algorithm was evaluated by solving three weight minimization benchmark truss structures with 72, 200, and 582 bars, including discrete variables. The material density and modulus of elasticity of the problems are given in Table 1.

The results obtained by IDEACO are compared with those of some other popular meta-heuristic methods, presented recently in the literature. These methods are selected among various metaheuristic for evaluation considering their high computational efficiency, quality of optimal solution, and superiority of performance of the proposed method.

Table 1. Main properties of benchmark truss structures.

Structure	72 bar	200 bar	582 bar
Modulus of elasticity (*Msi*)	10	30	29
Material density (lb/in^3)	0.1	0.283	0.283

4.1. 72-Bar Spatial Truss Structure

The layout of 72bar spatial truss structure depicted in Figure 4. This example has been investigated in [3,4,10,14,21,26]. The members of this structure are categorized in16 groups as follows:

(1) A_1- A_4, (2) A_5- A_{12}, (3) A_{13}- A_{16}, (4) A_{17}- A_{18}, (5) A_{19}- A_{22}, (6) A_{23}- A_{30}, (7) A_{31}- A_{34}, (8) A_{35}- A_{36}, (9) A_{37}- A_{40}, (10) A_{41}- A_{48}, (11) A_{49}- A_{52}, (12) A_{53}- A_{54}, (13) A_{55}- A_{58}, (14) A_{59}- A_{66}, (15) A_{67}- A_{70}, (16) A_{71}- A_{72}.

Two optimization cases were implemented; the discrete design variables of the cross-sectional area in both cases can be selected from the following:

Case (*i*): 0.1,0.2, 0.3, 0.4, 0.5, 0.6, 0.7, 0.8, 0.9, 1.0, 1.1, 1.2, 1.3, 1.4, 1.5, 1.6, 1.7, 1.8, 1.9, 2.0, 2.1, 2.2, 2.3, 2.4, 2.5, 2.6, 2.7, 2.8, 2.9, 3.0, 3.1, 3.2 (in^2).

Case (*ii*): The discrete design variables are selected from the available cross-sectional areas of the AISC code, listed in Table 2.

In Table 3; the loading condition of 72 bar truss structure is presented. The maximum tension or compression stress applied in members must not exceed $\pm 25 ksi$ ($\pm 172.38 MPa$). The displacement limitation of nodes is± 0.25 *in* (6.35*mm*) in all coordinate directions.

The results of 72 bar truss structure are shown in Tables 4 and 5 for case (*i*) and case (*ii*) respectively.In Table 4, it can be illustrated in Case (*i*) the best solution is achieved using IDEACO that is better than GA, HS, and HPSO. Although it is the same as DHPACO, DE, and HHS.

Table 5 shows that in Case (*ii*), the results obtained using IDEACO is better than previously published works such as GA, DHPSACO, and DE.

Table 2. The available cross-sectional areas for 72 bar truss structure (case (*ii*)).

No.	in^2	mm^2	No.	in^2	mm^2	No.	in^2	mm^2	No.	in^2	mm^2
1	0.111	71.613	17	1.563	1008.385	33	3.840	2477.414	49	11.500	7419.340
2	0.141	90.968	18	1.620	1045.159	34	3.870	2496.769	50	13.500	8709.660
3	0.196	126.451	19	1.800	1161.288	35	3.880	2503.221	51	13.900	8967.724
4	0.250	161.290	20	1.990	1283.868	36	4.180	2696.769	52	14.200	9161.272
5	0.307	198.064	21	2.130	1374.191	37	4.220	2722.575	53	15.500	9999.98
6	0.391	252.258	22	2.380	1535.481	38	4.490	2896.768	54	16.000	10322.56
7	0.442	285.161	23	2.620	1690.319	39	4.590	2961.284	55	16.900	10903.20
8	0.563	363.225	24	2.630	1696.771	40	4.800	3096.768	56	18.800	12129.01
9	0.602	388.386	25	2.880	1858.061	41	4.970	3206.445	57	19.900	12838.68
10	0.766	494.193	26	2.930	1890.319	42	5.120	3303.219	58	22.000	14193.52
11	0.785	506.451	27	3.090	1993.544	43	5.740	3703.218	59	22.900	14774.16
12	0.994	641.289	28	3.130	2019.351	44	7.220	4658.055	60	24.500	15806.42
13	1.000	645.160	29	3.380	2180.641	45	7.970	5141.925	61	26.500	17096.74
14	1.228	792.256	30	3.470	2238.705	46	8.530	5503.215	62	28.000	18064.48
15	1.266	816.773	31	3.550	2290.318	47	9.300	5999.988	63	30.000	19354.80
16	1.457	939.998	32	3.630	2341.931	48	10.850	6999.986	64	33.500	21612.86

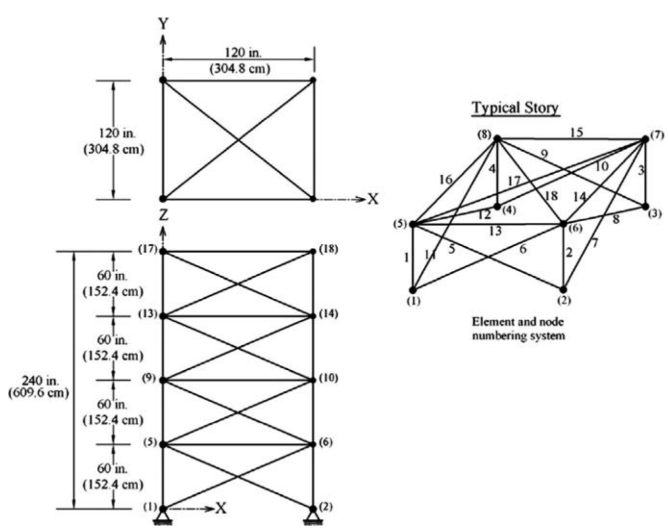

Figure 4. The layout of the spatial 72 bar truss structure

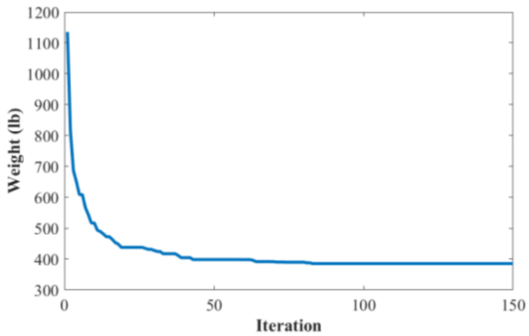

Fig. 5. Convergence curves of the spatial 72 bar truss structure for case (*i*).

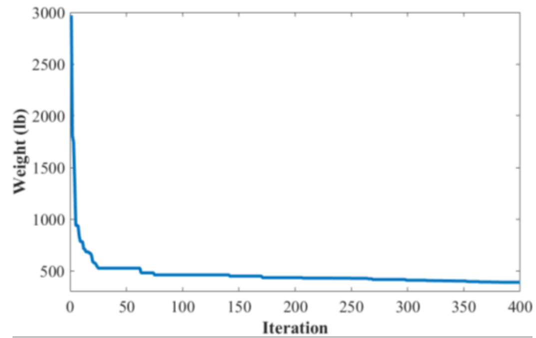

Fig. 6. Convergence curves of the spatial 72 bar truss structure for case (ii).

Table 3. Loading condition for 72 bar truss structure

Load case	nodes	P_x *kips (kN)*	P_y *kips (kN)*	P_z *kips (kN)*
1	17	5.0 (22.24)	5.0 (22.24)	-5.0 (-22.24)
2	17	0.0 (0.00)	0.0 (0.00)	-5.0 (-22.24)
	18	0.0 (0.00)	0.0 (0.00)	-5.0 (-22.24)
	19	0.0 (0.00)	0.0 (0.00)	-5.0 (-22.24)
	20	0.0 (0.00)	0.0 (0.00)	-5.0 (-22.24)

Table 4. Comparison of IDEACO results with literature for the 72-bar truss structure (case (*i*)).

Element Group	GA [26]	HS [4]	HPSO [10]	DHPSACO [14]	DE [21]	HHS [3]	IDEACO
1	1.5	1.9	2.1	1.9	2	1.9	2
2	0.7	0.5	0.6	0.5	0.5	0.5	0.5
3	0.1	0.1	0.1	0.1	0.1	0.1	0.1
4	0.1	0.1	0.1	0.1	0.1	0.1	0.1
5	1.3	1.4	1.4	1.3	1.3	1.3	1.3
6	0.5	0.6	0.5	0.5	0.5	0.5	0.5
7	0.2	0.1	0.1	0.1	0.1	0.1	0.1
8	0.1	0.1	0.1	0.1	0.1	0.1	0.1
9	0.5	0.6	0.5	0.6	0.5	0.6	0.5
10	0.5	0.5	0.5	0.5	0.5	0.5	0.5
11	0.1	0.1	0.1	0.1	0.1	0.1	0.1
12	0.2	0.1	0.1	0.1	0.1	0.1	0.1
13	0.2	0.2	0.2	0.2	0.2	0.2	0.2
14	0.5	0.5	0.5	0.6	0.6	0.6	0.6
15	0.5	0.4	0.3	0.4	0.4	0.4	0.4
16	0.7	0.6	0.7	0.6	0.6	0.6	0.6
Best (*lb*)	400.66	387.94	388.94	385.54	385.54	385.54	385.54
Average (*lb*)						386.040	386.096
Stdev (*lb*)						1.155	0.6774
No. of analyses		16044	50000			5000	6000

Table 5. Comparison of IDEACO results with literature for the 72-bar truss structure (case (*ii*))

Element Group	GA [26]	DHPSACO [14]	DE [21]	IDEACO
1	0.196	1.8	2.13	1.99
2	0.602	0.442	0.442	0.563
3	0.307	0.141	0.111	0.111
4	0.766	0.111	0.111	0.111
5	0.391	1.228	1.457	1.228
6	0.391	0.563	0.563	0.442
7	0.141	0.111	0.111	0.111
8	0.111	0.111	0.111	0.111
9	1.8	0.563	0.442	0.563
10	0.602	0.563	0.563	0.563
11	0.141	0.111	0.111	0.111
12	0.307	0.25	0.111	0.111
13	1.563	0.196	0.196	0.196
14	0.766	0.563	0.563	0.563
15	0.141	0.442	0.307	0.391
16	0.111	0.563	0.563	0.563
Best (*lb*)	427.203	393.38	391.329	389.33
Average (*lb*)				390.31
Stdev (*lb*)				1.010
No. of analyses				10000

Figures 5 and 6 show the comparison of convergence curves for 72 bar truss structure at case (i) and case (ii) respectively.

In Figures 7 and 8, the comparison of the allowable and existing constraints such as stress ratio ($\frac{\sigma_i}{\sigma_i^{all}}$) for 72 bar truss structure was shown by using IDEACO for case (i) and case (ii) respectively.

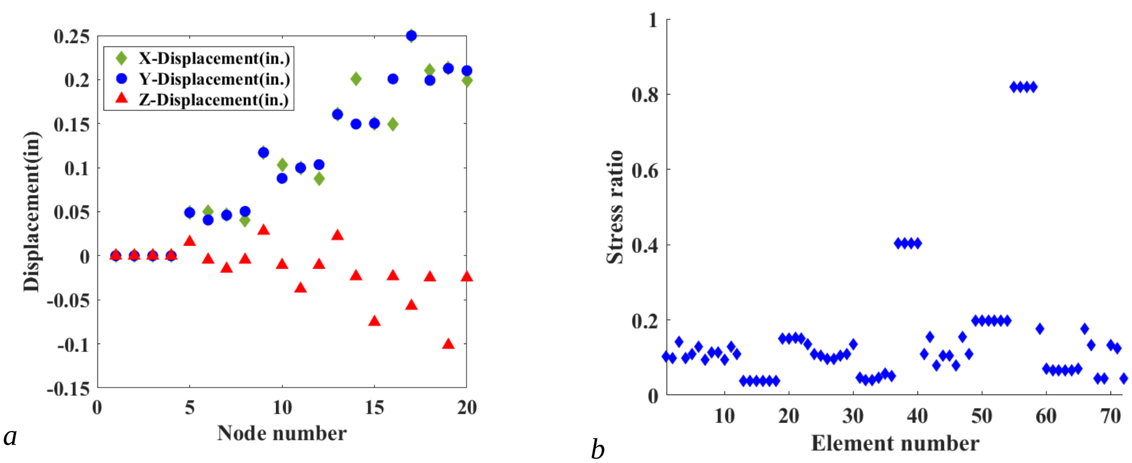

a *b*

Fig. 7. Comparison of the allowable and existing constraints for 72 bar truss structure, case (*i*): *a*) Displacement in all coordinate direction, *b*) stress ratio.

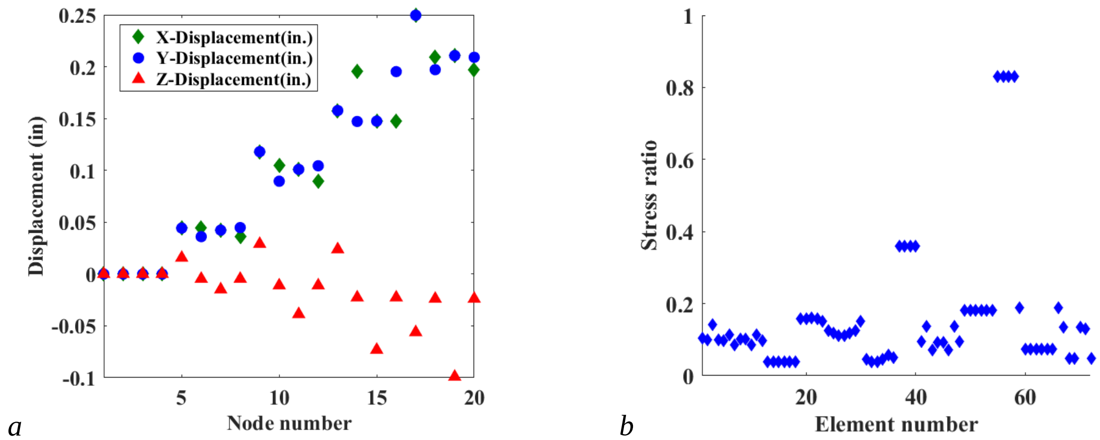

Fig. 8. Comparison of the allowable and existing constraints for 72 bar truss structure, case (*ii*): *a*) Displacement in all coordinate direction, *b*) stress ratio.

4.2. 200 Bar Planar Truss Structure

The third example considered throughout this paper is the 200-bar planar truss structure shown in Figure 9. This structure is investigated as a large-scale, size optimization problem in some recent papers [3, 27, 28, 29]. The stress limitation on members is ± 10 *ksi* ($\pm 68.95 MPa$).

In this structure, the members are divided into 29 groups that described in Table 6. The discrete design variables of the cross-sectional area in both cases can be selected from the following:

0.1, 0.347, 0.44, 0.539, 0.954, 1.081, 1.174, 1.333, 1.488, 1.764, 2.142, 2.697, 2.8, 3.131, 3.565, 3.813, 4.805, 5.952, 6.572, 7.192, 8.525, 9.3, 10.85, 13.33, 14.29, 17.17, 19.18, 23.68, 28.08, 33.7 (*in*).

This structure was subjected to three loading conditions presented in Table 7.

Table 8 presents the statistical results obtained by the IDEACO algorithm and the other optimization methods.

It is obvious; that IDEACO reached the superior results compared to other methods, in best, average and standard deviation which are 26831.22, 27634.24 and 371.03*lb* respectively, in over 12000 numbers of analyses. Figure10 depicts the convergence curves of 200 bar truss structure.

In Figure11, for 200 bar truss structure, the comparison of the allowable stress constraints for elements and displacement of nodes were shown by using IDEACO.

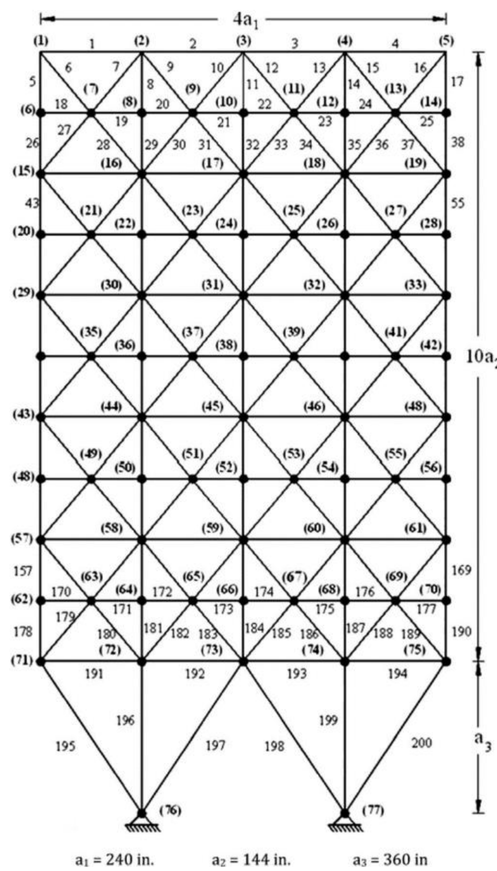

Figure 9. The layout of the 200-bar truss structure

Table 6. The design variables in the 200 bar truss structure

Element Groups	Number of truss elements
1	1, 2, 3, 4
2	5, 8, 11, 14, 17
3	19, 20, 21, 22, 23, 24
4	18, 25, 56, 63, 94, 101, 132, 139, 170, 177,
5	26, 29, 32, 35, 38
6	6, 7, 9, 10, 12, 13, 15, 16, 27, 28, 30, 31, 33, 34, 36, 37
7	39, 40, 41, 42
8	43, 46, 49, 52, 55
9	57, 58, 59, 60, 61, 62
10	64, 67, 70, 73, 76
11	44, 45, 47, 48, 50, 51, 53, 54, 65, 66, 68, 69, 71, 72, 74, 75
12	77, 78, 79, 80
13	81, 84, 87, 90, 93
14	95, 96, 97, 98, 99, 100
15	102, 105, 108, 111, 114
16	82, 83, 85, 88, 89, 91, 92, 103, 104, 106, 107, 109, 110, 112, 113
17	115, 116, 117, 118
18	119, 122, 125, 128, 131
19	133, 134, 135, 136, 137, 138
20	140, 143, 146, 149, 152
21	120, 121, 123, 124, 126, 127, 129, 130, 141, 142, 144, 145, 147, 148, 150, 151
22	153, 154, 455, 156
23	157, 160, 163, 166, 169
24	171, 172, 173, 174, 175, 176
25	178, 181, 184, 187, 190
26	158, 159, 161, 162, 164, 165, 167, 168, 179, 180, 182, 183, 185, 186, 188, 189
27	191, 192, 193, 194
28	195, 197, 198, 200
29	196, 199

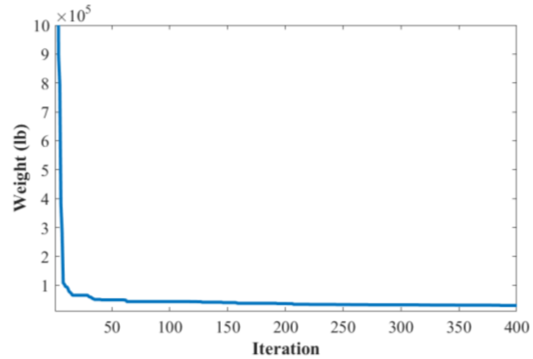

Fig. 10. Convergence curve of the 200-bar truss structure

Table 7. Loading condition for the 200-bar truss structure.

Load case	Force *kips*	direction	Node number
1	1	X	1, 6, 15, 20, 29, 34, 43, 48, 57, 62,71
2	-10	Y	1-6, 8, 10, 12, 14, 16-20, 22, 24, 26, 28-34, 36, 38, 40, 42-48, 50, 52, 54, 56-62, 64, 66, 68, 70-75
3			Load cases (1) and (2) together

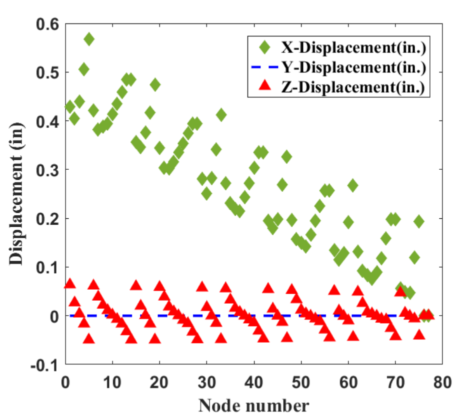

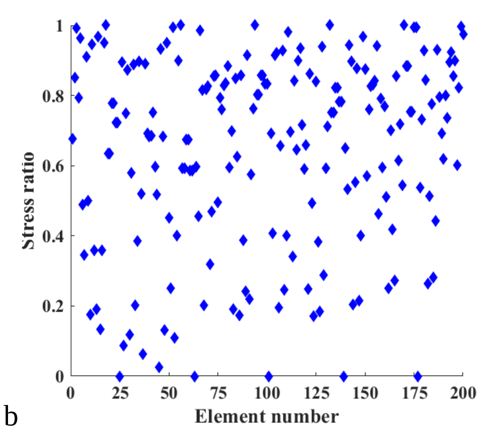

Fig. 11. Comparison of the allowable stress constrains and displacement nodes for 200 bar truss structure, a) Displacement in all coordinate direction, b) stress ratio.

Table 8. Comparison of IDEACO results with literature for the 200-bar truss structure

Variables	ESASS [27]	ADS [28]	HHS [3]	ADDE [29]	IDEACO
1	0.1	0.1	0.1	0.1	0.1
2	0.954	0.954	0.954	0.954	0.954
3	0.1	0.347	0.1	0.1	0.1
4	0.1	0.1	0.1	0.1	0.1
5	2.142	2.142	2.142	2.142	2.142
6	0.347	0.347	0.347	0.347	0.347
7	0.1	0.1	0.1	0.347	0.1
8	3.131	3.131	3.131	3.131	3.131
9	0.1	0.1	0.1	0.1	0.347
10	4.805	4.805	4.805	4.805	4.805
11	0.347	0.44	0.44	0.539	0.347
12	0.1	0.1	0.347	0.1	0.1
13	5.952	5.952	5.952	5.952	5.952
14	0.1	0.1	0.347	0.1	0.1
15	6.572	6.572	6.572	6.572	6.572
16	0.44	0.539	0.954	0.440	0.539
17	0.539	0.1	0.347	0.539	0.347
18	7.192	8.525	8.525	8.525	8.525
19	0.44	0.539	0.1	0.347	0.44
20	8.525	9.3	9.3	9.3	9.3
21	0.954	0.954	1.081	0.954	0.954
22	1.174	0.1	0.347	0.1	0.1
23	10.85	10.85	13.33	13.33	13.33
24	0.44	0.954	0.954	0.1	0.1
25	10.85	13.33	13.33	13.33	13.33
26	1.764	1.333	1.764	0.954	0.954
27	8.525	7.192	3.813	5.952	5.952
28	13.33	10.85	8.525	10.85	10.85
29	13.33	14.29	17.17	14.29	14.29
Best (*lb*)	28,075.49	27,190.49	27,163.59	26960.152	26831.22
Average (*lb*)			28,159.59	27969.510	27634.24
Stdev (*lb*)			1149.91	422.130	371.03
No. of analyses	11,156	5000	5000	6189	12,000
Constraint violation	None	None	%36.42	None	None

4.3. 582 Bar Planar Truss Structure

In Figure 12, the layout of 582bar spatial truss structure was presented. In this structure, the members are divided into 32 groups, as showed in Figure 12. This example has been investigated in [14, 21, 30, 31].

The discrete design variables of the cross-sectional area can be selected from 140 economic standard steel W-shape profile list based on the area and radius of gyration properties. The lower and upper bounds on cross-sectional areas of all elements can be taken as between 39.74 and 1378.09 cm^2 (6.16 and 215 in^2).

This tower structure was subject to a single load case, the lateral loads of 5 *kN* (1.12 *kips*) and 30 *kN* (6.74 *kips*) applied in both *x* and *y* directions and in the *z*-direction at all nodes, respectively. The nodal displacement of nodes must not exceed 3.15 in (80 mm).The stress limitations of the members are considering, according to ASD-AISC as Eq. 16.

$$\begin{cases} \sigma_i^T = 0.6F_y\sigma_i > 0 \\ \quad \sigma_i^C\sigma_i < 0 \end{cases} \tag{16}$$

Where σ_i^C can be computed according to the slenderness ratio as Eqs. 17 and 18.

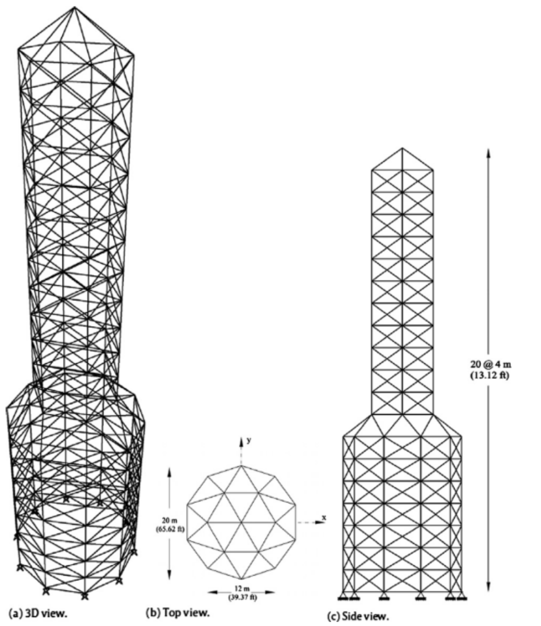

Fig. 12. The layout of the 582-bar spatial truss structure.

$$\sigma_i^C = \begin{cases} \dfrac{\left(\frac{1-\lambda_i^2}{2C_i^2}\right)F_y}{\left(\frac{5}{3}+\frac{3\lambda_i}{8C_c}-\frac{\lambda_i^3}{8C_c^3}\right)} \lambda_i < C_c \\ \dfrac{12\pi^2 E}{23\lambda_i^2} \lambda_i \geq C_c \end{cases} \quad (17)$$

$$C_c = \sqrt{\frac{2\pi^2 E}{F_y}} \quad (18)$$

Where E, λ and F_y are the modulus of elasticity, the slenderness ratio ($\lambda_i = k_i L_i / r_i$) and the yield stress (248 *MPa* (36*ksi*)) according to ASD-AISD respectively. The slenderness ratio divides the elastic and inelastic buckling regions by C_c.L_i is the slenderness ratio, r_i, and $k_i$are radius of gyration and effective length factor, respectively.

The slenderness ratio must not exceed 300 and 200 for tension and compression members, respectively. If for compression members, the slenderness ratio was more than 200, the value of stress in these members should be less than the value calculated by $\frac{12\pi^2 E}{23\lambda_i^2}$.

This tower structure is analyzed for two different cases as follows.

case (*i*): maximum number of iteration in the optimization process is considered 1000.

case (*ii*): maximum number of iteration in the optimization process is considered 2000.

The optimization results of 582 bar truss structure are shown in Table 9. The results obtained by IDEACO are the superiors compared with other methods, in best, average, worst, standard deviation, and number of analysis in both cases.

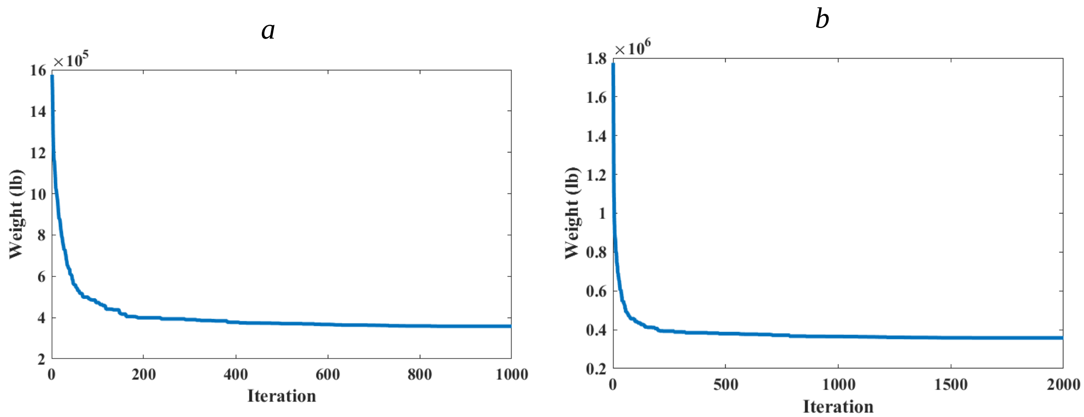

Fig. 13. Convergence curves of the spatial 582 bar truss structure, a. case (*i*), b. case (*ii*).

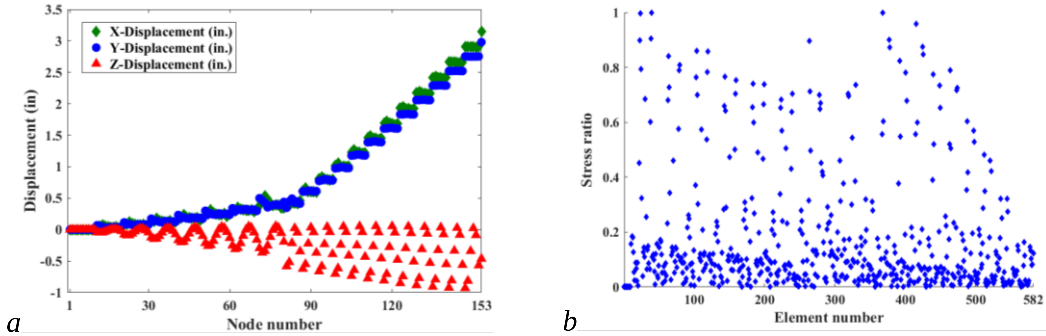

Fig. 14. Comparison of the allowable stress constrains and displacement nodes for 582 bar truss structure, *a*) Displacement in all coordinate direction, *b*) stress ratio.

Table9. Comparison of IDEACO results with literature for the 582-bar truss structure.

	Case (*i*)					Case (*ii*)		
Variables	PSO [30]	ABC [31]	DHPSACO [14]	DE [21]	IDEACO	ABC [31]	DE [21]	IDEACO
1	W8×21	W8×22	W8×24	W8×21	W8×21	W8×22	W8×21	W8×21
2	W12×79	W12×97	W12×72	W12×96	W14×90	W10×78	W27×94	W14×90
3	W8×24	W8×25	W8×28	W8×24	W8×024	W8×25	W8×24	W8×24
4	W10×60	W12×59	W12×58	W12×58	W10×60	W14×62	W12×58	W14×61
5	W8×24	W8×24	W8×24	W8×24	W8×24	W8×24	W8×24	W8×24
6	W8×21	W8×21	W8×24	W8×21	W8×21	W8×21	W8×21	W8×21
7	W14×48	W12×46	W10×49	W12×45	W10×49	W12×51	W12×50	W14×48
8	W8×24	W8×24	W8×24	W8×24	W8×24	W8×24	W8×24	W8×24
9	W8×21	W8×21	W8×24	W8×21	W8×21	W8×21	W8×21	W8×21
10	W10×45	W12×46	W12×40	W12×45	W14×43	W10×50	W12×45	W10×45
11	W8×24	W8×22	W12×30	W8×21	W8×21	W8×25	W8×21	W8×21
12	W10×68	W12×66	W12×72	W12×65	W16×67	W10×69	W12×72	W16×67
13	W14×74	W10×77	W18×76	W10×77	W18×76	W18×77	W14×74	W14×74
14	W14×48	W10×49	W10×49	W10×49	W10×45	W14×49	W12×50	W10×45
15	W18×76	W14×83	W14×82	W14×82	W14×74	W10×78	W10×68	W18×76
16	W8×31	W8×32	W8×31	W8×31	W8×31	W8×32	W8×31	W8×31
17	W16×67	W12×53	W14×61	W10×60	W16×67	W21×62	W14×61	W16×67
18	W8×24	W8×24	W8×24	W8×24	W10×22	W8×24	W8×24	W10×22
19	W8×21	W8×21	W8×21	W8×21	W8×21	W8×21	W8×21	W8×21
20	W8×40	W16×36	W12×40	W12×45	W14×43	W14×43	W14×43	W14×43
21	W8×24	W8×24	W8×24	W8×21	W8×21	W8×24	W8×21	W8×21
22	W8×21	W10×22	W14×22	W8×21	W8×21	W8×21	W8×21	W8×21
23	W10×22	W10×22	W8×31	W10×22	W8×24	W8×24	W6×25	W8×24
24	W8×24	W6×25	W8×28	W8×21	W8×21	W8×24	W8×21	W8×21
25	W8×21	W8×21	W8×21	W8×21	W8×21	W8×21	W8×21	W8×21
26	W8×21	W8×21	W8×21	W8×21	W8×21	W8×21	W8×21	W8×21
27	W8×24	W8×24	W8×24	W8×21	W8×21	W8×24	W8×21	W8×21
28	W8×21	W8×21	W8×28	W8×21	W8×21	W8×21	W8×21	W8×21
29	W8×24	W8×22	W16×36	W8×21	W8×21	W8×21	W8×21	W8×21
30	W8×21	W10×23	W8×24	W8×21	W8×21	W8×21	W8×21	W8×21
31	W8×21	W8×25	W8×21	W8×21	W8×21	W8×24	W8×21	W8×21
32	W8×24	W6×26	W8×24	W8×21	W8×21	W8×24	W8×21	W8×21
Best (*lb*)	363795.7	368484.1	380982.7	360367.8	357933.4	365906.3	360143.3	357906.6
Average (*lb*)	365124.9	370178.6		364404.7	359357.6	366088.4	362207.1	358830.8
Worst (*lb*)	370159.1	373530.3		371922.1	361499.0	369162.2	367512.2	360534.2
Stdev (*lb*)					1176.40			1133.24
No. of analyses	50000	50000	8500	25000	20000	100000	50000	40000

In case (*i*), the best design in IDEACO algorithm was 1.64%, 2.95%, 6.44%, and 0.68% lighter than PSO, ABC, DHPSACO, and DE respectively. In case (*ii*), the best design in IDEACO algorithm was 2.24% and 0.63% lighter than ABC and DE respectively.

Figure 13 depicts the convergence curve of 582 bar spatial truss structure in both cases.

In Figure 14, for 582 bar truss structure, the comparison of the allowable stress constraints for elements and displacement of nodes was shown by using IDEACO.

5. Conclusion

In this paper, a new hybrid optimization algorithm was presented, including dolphin echolocation and ant colony optimization. This algorithm can be applied for discrete sizing optimization problems such as truss structures. At first, the DE was improved as called IDE, and then it is hybridized with ant colony optimization algorithm to use solution benchmark structural optimization problems. The performance and efficiency of IDEACO were tested extensively using four benchmark truss structure optimization problems. The comparison of the numerical result received by IDEACO and other optimization methods are presented. These results verify the efficiency, effectiveness, and robustness of the proposed method.

The IDEACO algorithm yielded better results than optimization methods applied for comparison in convergence capability and optimum design. Almost in all design problems, the proposed algorithm reached a result that is better than or similar to literature and needed much fewer structural analyses. So, hybridization of the IDE and ACO not only may lead to a balance between exploitation and exploration but also improve convergences to optimum design. IDEACO is the desired method for solving complex problems, and the hybrid method is surely an issue to be studied in future researches.

REFERENCES

[1] Hare, W., Nutini, J., Tesfamariam, S. (2013). “A survey of non-gradient optimization methods in structural engineering.” Advances in Engineering Software, Vol. 59, pp. 19–28.

[2] Leandro Fleck Fadel Miguel, L. F. F., Rafael Holdorf Lopez, R. H., Miguel, L. F. F. (2013). “Multimodal size, shape, and topology optimisation of truss structures using the Firefly algorithm.” Advances in Engineering Software, Vol. 56, pp. 23–37.

[3] Min-Yuan Cheng, M. Y., Prayogo, D. Yu-Wei W., Lukito, M. M., (2016). “A Hybrid Harmony Search algorithm for discrete sizing optimization of truss structure.” Automation in Construction, Vol. 69, pp. 21–33.

[4] Lee, K. S., Geem, Z. W., Lee, S. H., Bae, K. W., (2005). “The harmony search heuristic algorithm for discrete structural optimization.” Engineering Optimization, Vol. 37, Issue 7, pp. 663–684.

[5] Ghoddosian, A., Sheikhi, M., (2013). “Metaheuristic optimization methods in engineering.” Semnan University Press.

[6] Kaveh, A., Mahdavi, V. R., (2015). “A hybrid CBO–PSO algorithm for optimal design of truss structures with dynamic constraints.” Applied Soft Computing, Vol. 34, pp. 260–273.

[7] Rajeev, S., Krishnamoorthy, C. S. (1992). “Discrete optimization of structures using genetic algorithms.” Journal of Structural Engineering, Vol. 118, Issue 5, pp. 1233-1250.

[8] Bennage, W. A. Dhingra, A. K., (1995). “Single and multi-objective structural optimization in discrete continuous variables using simulated annealing.” International Journal for Numerical

Methods in Engineering, Vol. 38, Issue 16, pp. 2753-2773.

[9] Camp, C. V., Bichon, B. J., (2004). "Design of space trusses using ant colony optimization." Engineering Optimization, Vol. 130, Issue 5, pp. 741-751.

[10] Li, L. J., Huang, Z. B., Liu, F., (2009). "A heuristic particle swarm optimization method for truss structures with discrete variables." Computer Structures., Vol. 87, Issue 7, pp. 435-443.

[11] Eskandar, H., Sadollah, A., Bahreininejad, A., Hamdi, M., (2012). "Water cycle algorithm – A novel metaheuristic optimization method for solving constrained engineering optimization problems." Computers Structures, Vol. 110, pp. 151–166.

[12] Sadollah, A., Bahreininejad, A., Eskandar, H., Hamdi, M., (2012). "Mine blast algorithm for optimization of truss structures with discrete variables." Computers Structures, Vol. 102, pp. 49–63.

[13] Sheikhi, M., Delavar, M., Arjmand, M., (2016). "Time evolutionary optimization: A new meta-heuristic optimization algorithm." Proceedings of the 4th International Congress on Civil Engineering, Architecture and Urban Development, Shahid Beheshti University, Tehran, Iran.

[14] Kaveh, A., Talatahari, S., (2009). "Particle swarm optimizer, ant colony strategy and harmony search scheme hybridized for optimization of truss structures." Computer Structures, Vol. 87, pp. 267-283.

[15] Kaveh, A., Talatahari, S., (2012). "A hybrid CSS and PSO algorithm for optimal design of structures." Structural Engineering and Mechanics, Vol. 42, Issue 6, pp.783-797.

[16] Sheikhi, M., Ghoddosian, A., (2013). "A hybrid imperialist competitive ant colony algorithm for optimum geometry design of frame structures, Structural Engineering and Mechanics." Vol. 46, Issue 3, pp. 403-416.

[17] Sadollah, A., Eskandar, H., Bahreininejad, A., Kim, J. H., (2015). "Water cycle, mine blast and improved mine blast algorithms for discrete sizing optimization of truss structures." Computers Structures, Vol. 149, pp. 1–16.

[18] Shojaee, S., Arjomand, M., Khatibinia, M., (2013). "A hybrid algorithm for sizing and layout optimization of truss structures combining discrete PSO and convex approximation," International Journal ofOptimization in Civil Engineering, Vol 3, Issue 1, pp. 57-83.

[19] Kaveh, A., Mahdavi, V. R., (2015). "A hybrid CBO–PSO algorithm for optimal design of truss structures with dynamic constraints." Applied Soft Computing, Vol. 34, pp. 260–273.

[20] Lotfi, H., Ghoddosian, A., (2015). "Size and Shape Optimization of Two-Dimensional Trusses Using Hybrid Big Bang-Big Crunch Algorithm." International journal of mechatronics, electrical and computer technology, Vol. 5, Issue 14, PP. 1987-1998.

[21] Kaveh, A., Farhoudi, N., (2013). "A new optimization method: Dolphin echolocation." Advances in Engineering Software, Vol. 59, pp. 53–70.

[22] Kaveh, A., Hosseini, P., (2014). "A simplified dolphin echolocation optimization method for optimum design of trusses." International Journal of Optimization in Civil Engineering, Vol. 4, Issue 3, pp. 381-397.

[23] Kaveh, A., IlchiGhazaan, M., (2014). "Enhanced colliding bodies optimization for design problems with continuous and discrete."Advances in Engineering Software, Vol. 77, pp. 66–75.

[24] Socha, K., Blum, Ch., (2007). "An ant colony optimization algorithm for continuous optimization: application to feed-forward neural network training." Neural Computing and Applications, Vol. 16, pp. 235-247.

[25] Coelllo C. A. C., (2002). "Theoretical and numerical constraint-handling techniques used with evolutionary algorithms: a survey of the state of the art." Computer

Methods in Applied Mechanics and Engineering, Vol.191, pp. 1245–1287.

[26] Wu, S. J, Chow, P. T. (1995). “Steady-state genetic algorithms for discrete optimization of trusses.” Computer Structure, Vol. 56, pp. 979–91.

[27] Azad, S. K., Hasançebi, O., (2014). “An elitist self-adaptive step-size search for structural design optimization.” Applied Soft Computing, Vol. 19, pp. 226-235.

[28] Azad, S. K., Hasançebi, O., (2015). “Discrete sizing optimization of steel trusses under multiple displacement constraints and load cases using guided stochastic search technique.” Structural and Multidisciplinary Optimization, Vol. 52, Issue 2, pp. 383-404.

[29] Pham, A. H., (2016). “Discrete optimal sizing of truss using adaptive directional differential evolution.” Advances in Computational Design, Vol. 1, Issue 3, pp. 275-296.

[30] Hasancebi, O., Carbas, S., Dogan, E., Erdal F., Saka M. P. (2009). “Performance evaluation of metaheuristic search techniques in the optimum design of real size pin jointed structures.” Computer Structures, Vol. 87, Issue 5, pp.284–302.

[31] Sonmez, M., (2011). “Discrete optimum design of truss structures using artificial bee colony algorithm.” Structural and Multidisciplinary Optimization, Vol. 43, pp. 85–97.